Article.

Disinfection of Digestate Effluents Using Photocatalytic Nano-Filtration

Afroditi G. Chioti [1], Georgia Sarikaki [1], Vasiliki Tsioni [1], Eleni Kostopoulou [1], George Romanos [2], Polycarpos Falaras [2] and Themistoklis Sfetsas [1*]

[1] QLAB Private Company, Research & Development, Quality Control and Testing Services, 57008 Thessaloniki, Greece
[2] Institute of Nanoscience and Nanotechnology, National Center of Scientific Research "Demokritos", Agia Paraskevi, 15310 Athens, Greece
* Correspondence: t.sfetsas@q-lab.gr; Tel.: +30-2310-784712

Abstract: The physiological characteristics of liquid digestate retrieved from various biogas plants based in northern Greece are presented. Preliminary photocatalysis experiments on inoculated liquid digestate sampled showed that disinfection is possible when pre-treated digestate with a combination of centrifuge-flocculation-μFiltration after 5.5 hours of 0.7g/L suspended TiO2 under UVA illumination for the experimental conditions is used. A novel design photocatalytic nanofiltration reactor was implemented for disinfection experiments on pre-treated liquid digestate, giving promising results. This work sets the basis for the efficient operation and engineering application of technology collaboration with photocatalysis as the final step for liquid digestate sanitation and reusable water recovery.

Keywords: disinfection; indicator pathogens; TiO_2 photocatalysis; photocatalytic nanofiltration reactor; membrane filtration; anaerobic digestion; liquid digestate

1. Introduction

Anaerobic digestion (AD) is a biochemical process conducted in an anaerobic digester, wherein a diverse community of microorganisms converts complex organic matter (OM) into biogas and digestate (WD) under controlled conditions without the presence of oxygen [1]. AD serves as a widely employed technique for effectively diminishing the volume of various biomass sources, including the organic fraction of industrial waste, energy crops, agricultural residues, and forestry remnants, while simultaneously recovering renewable energy. [2, 3]. Despite being recognized as a highly favorable waste treatment technology, particularly from an environmental standpoint, AD does not achieve complete waste stabilization [4].

Whole digestate (WD) can be mechanically separated into two fractions: a solid fraction called solid fibrous digestate (SFD), characterized by higher organic matter (OM), phosphorus (P) and potassium (K) content, and a liquid fraction called liquid digestate (LD), which exhibits greater nitrogen (N). As a result, the liquid fraction holds greater potential as a fertilizer, while the solid fraction exhibits greater potential for amending soil composition [5]. However, it is important to note that WD derived from agricultural biogas plants does not meet the necessary soil regulations. Consequently, further treatment through recycling is required to mitigate potential environmental risks [6].

Pathogenic microorganisms including *Escherichia coli*, *Enterococcus faecalis*, *Salmonella* spp., *Listeria monocytogenes*, *Clostridium perfringens* and zoonotic viruses like porcine parvovirus, which are generally not problematic during the AD of animal wastes such as cattle, pig, poultry, and sheep manure [7, 8], have the ability to survive the digestion process and persist in the WD especially in mesophilic conditions [9]. As WD can serve as a potential vehicle for pathogen transmission from agricultural land to humans through the

 doi:10.20944/preprints202305.2203.v1

food chain, it is crucial to ensure proper sanitation practices. The sanitation of WD relies on multiple factors, including the quality of substrates fed into the reactor, reactor performance, digestion temperature, slurry retention time, pH, and NH_3 concentration. Different pre-treatment methods, such as pasteurization [10], chlorine treatment, UV-light exposure, ozone treatment [11], and high-pressure treatment within a vessel [12], can be employed to reduce the pathogen load in the final WD effluent.

The primary objective of effective WD sanitation is to achieve a reduction in the concentration of *Enterococcus faecalis* or *Salmonella senftenberg* by a factor of 5 $\log_{10}$ and thermal-resistant viruses by a factor of 3 $\log_{10}$. *Enterococcus faecalis* (a Gram-positive bacterium) and *Escherichia coli* (a Gram-negative bacterium) are commonly used as indicator microorganisms to evaluate the efficacy of the sanitation process. *Enterococcus faecalis* has also been selected as an indicator bacterium according to EU regulation No. 142/2011 [13]. While the thermal inactivation of pathogens has been extensively studied on a laboratory scale, caution must be exercised when extrapolating the results to large-scale systems. Factors such as uneven heating, fluctuating temperatures, and the shielding properties of solids can affect the required exposure time for pathogen inactivation. Therefore, further investigation is necessary to transfer laboratory findings to full-scale systems [14].

Apart from conventional thermal pasteurization technologies, alternative methods, such as electro-technology, microwave treatment, pressurization, ultrasound treatment, and chemical treatments have the potential to significantly reduce bacterial populations and simultaneously increase methane (CH_4) yield. However, the performance of these alternative technologies varies depending on the type of waste, operational parameters, and energy input [15]. It should be noted that certain spore-forming bacteria, such as *Clostridium* spp. and *Bacillus* spp., which are less sensitive to heat, may not be effectively reduced [9, 16] [17, 18]. This was also demonstrated in a study investigating the hygiene aspects of WD, where elevated levels of *Bacillus* spp. were detected, suggesting that neither the sanitation treatment nor the subsequent AD process affected the abundance of *Bacillus* spp. [19]. Another study examined liquid manures and WD from five biogas plants in France to assess the contamination by both sporulating (*Clostridium perfringens*, *Clostridioides difficile*, and *Clostridium botulinum*) and non-sporulating (*Escherichia coli*, *Enterococci*, *Salmonella* spp., *Campylobacter*, and *Listeria monocytogenes*) bacterial species. The authors concluded that spore-forming bacteria, as well as *Listeria monocytogenes*, *Salmonella* spp., and *Enterococci*, can persist during AD; however, the concentration of these pathogens in WD was similar to or lower than that in liquid manures [20]. Finally, as WD is often stored prior to application on agricultural land or distribution, there is a possibility of pathogen regrowth during storage [21]. Therefore, further treatment of WD is recommended to achieve more efficient pathogen reduction.

A highly efficient method known as advanced oxidation processes (AOPs) has emerged as a promising solution for eliminating organic pollutants from various sources, including water, on a large scale. AOPs facilitate the conversion of organic compounds into harmless by-products, such as CO_2 and H_2O, thereby ensuring their safe removal [22, 23]. By generating intermediate radicals, notably the hydroxyl radical (radical ·OH), AOPs exhibit exceptional reactivity, enabling them to effectively oxidize a wide range of organic molecules [24]. Commonly employed AOPs include ozonation, Fenton and photo-Fenton processes, photolysis, photocatalysis, and electrochemical methods, each offering distinct advantages [25-27]. Notably, photocatalysis has garnered significant attention due to its economical, efficient, environmentally friendly nature, coupled with its moderate reaction conditions. Due to its excellent catalytic reactivity, robust physical and chemical stability, non-toxic nature, and cost-effectiveness, the semiconductor TiO_2 has found extensive application as a photocatalyst [28, 29]. Nevertheless, only few research teams explored the application of photocatalysis on liquid digestate (LD).

Wang *et al.*, (2021, 2023) explored the effect of photocatalysis on the physicochemical properties of LD and the photocatalytic degradation of tetracyclines. They have found that under high pressure mercury lamp and under the optimum conditions (TiO_2 of 1.0 g/L,

 doi:10.20944/preprints202305.2203.v1

LD depth of 20 mm and photocatalytic time of 120 min), the removal of tetracycline, oxytetracycline, and chlortetracycline reached 94.99%, 88.92%, and 95.52%, respectively. LD from swine manure and 10% wastewater, was used after centrifugation. Average values of COD of the LD supernatant was 1576 ± 92 mg/L, TS was 3763 ± 39 mg/L, and turbidity was 179 ± 5 NTU [30]. In a more resent study, results showed minor effects on major nutrients, an increase in tryptophan substances, soluble microbial by-products, and a decrease in humic acid substances. The toxicity of the LD initially increased and then decreased, with improved seed germination and root growth after 2 hours of photocatalysis. Bacterial community richness, diversity, and evenness decreased, with a shift from *Firmicutes* to *Proteobacteria*. As expected, the physicochemical properties of the LD, such as pH, total solids, and chroma, significantly influenced the photocatalytic process [31]. This highlights the imperative to establish a pre-treatment protocol aimed at attaining targeted ranges for the physicochemical properties of WD. In these studies, the application of flocculation pre-treatment proved effective for that matter.

Yin *et al.* (2021) treated WD with a combination of membrane separation and photocatalysis for antibiotic removal [32]. Jin *et al.* (2019) found the photocatalytic degradation efficiency of norfloxacin for N-doped TiO_2 is approximately 11 mg/g [33]. The aim of this study is to serve as a reference for the use of combined membrane filtration technologies with additional treatment systems to treat antibiotic-containing wastes. Combined membrane process included a succession of paper filtration (PF), hollow-fiber membrane ultrafiltration (HF), nanofiltration (NF) and reverse osmosis (RO) that reduced turbidity of WD from 318,76 NTU to 0,36 NTU, COD from 746 mg/L to 3 mg/L and TSS from 2263 mg/L to 63 mg/L. Nevertheless, antibiotics were incompletely removed at each step of the membrane process. For the photocatalysis experiment, 500 mg/L of P25 was added to samples and subjected to 30 min of dark absorption prior to light exposure. A photocatalytic reactor was used (CEL-LBX, AULIGHT, Beijing) for the process, and Xe light was used as the light source. The total reaction time was 4 h. P25 was highly effective in removing the 10 antibiotics, including quinolones and tetracyclines, investigated in this study. It provided average removal rates of more than 90% for each antibiotic. Its highest removal rate was 99.9% in HF concentrate followed by 99.3% in digested slurry, 98.3% in PF permeate, 96.9% in NF permeate, 95.4% in HF permeate, 91.5% in RO permeate, and 89.9% in NF permeate. Similar results have been obtained for CIP, ENR, TE, and OTC [34-36] in deionized water, ultrapure water, or urban wastewater at the concentration of 5–10 mg/L. Although absorbents like fine halloysite exhibited higher removal efficiencies, photocatalysis can mineralize and reduce toxicity of antibiotics. Therefore, photocatalysis is considered the best method combined with each stage of membrane filtration.

The application of photocatalysis for WD sanitation has not been studied yet. The high total solid content in matrices like WD can pose challenges for photocatalysis, due to factors, such as reduced light penetration, hindered photocatalyst, contact with target pathogens, and potential catalyst fouling [37]. However, researchers have been investigating methods to overcome these challenges and optimize photocatalytic disinfection in such complex matrices [38-40].

Membrane technology can be employed to attenuate solids, thereby enhancing light transmission, and facilitating the feasibility of photocatalysis. The main drawbacks include the high upfront costs [41] and the tendency for membrane fouling and clogging, which can lead to decreased performance and significant operational expenses [42]. A comprehensive exploration has been conducted on a wide range of membrane processes for the treatment of WD; microfiltration [41, 43], ultrafiltration [44, 45], nanofiltration [46, 47], reverse osmosis [46, 47], and forward osmosis [42]. Microfiltration and ultrafiltration, two widely utilized membrane process technologies, are capable of concentrating particles and molecules ranging from 0.01 to 1 μm. These include various substances like pathogens (bacteria, viruses, etc.), organic macromolecules (proteins, carbohydrates, etc.), and minerals (clays, latex, etc.), which can be effectively separated using microporous

 doi:10.20944/preprints202305.2203.v1

membranes. These methods offer the advantage of operating at relatively low pressures (0.1 to 5 bar), resulting in reduced energy costs [48].

However, membrane technology generates a retentate with higher concentration of pollutants and pathogens compared to the original material that will also need special management before disposal. On the other hand, photocatalysis is commonly employed as ultra-thin photocatalytic coatings supported on transparent substrates and integrated into continuous flow systems. The purpose of this support is to mitigate the challenges associated with applying photocatalysis through batch processes, utilizing suspensions of photocatalytic powders. These challenges pertain to intricate procedures for separating and recovering photocatalytic nanoparticles from treated wastewater. When photocatalytic coatings are utilized, limitations in mass transfer, inadequate mixing, and brief contact times contribute to a moderate level of photocatalytic degradation performance. Additionally, an inherent drawback of stand-alone photocatalysis is the competitive interaction with organic matter, whether of natural or synthetic origin, which typically exists in WD and occupies the active adsorption sites on the surface of the photocatalyst. Therefore, novel, more advanced solutions that could effectively sanitised WD are needed [49].

In this context, a patented lab-scale reactor was configured for LD treatment [50], integrating photocatalysis and filtration in one reactor module. The efficiency of the hybrid photocatalytic nanofiltration reactor (PNFR) relied on several factors: (a) its ability to simultaneously irradiate numerous photocatalytic surfaces within the photocatalytic-membrane reactor module, while implementing the tangential flow-filtration process; (b) the disinfection capabilities achieved through the utilization of titania (TiO_2) photocatalysts and the photoinduced radical mechanism triggered by appropriate wavelength light illumination [51]; and (c) the concurrent retention of micropollutants by the nanoporous membranes [52] as described [53]. Until now, the PNFR has not been tested against common pathogens in LD.

In this study, we present the physicochemical characteristics of LD retrieved from various biogas plants based in northern Greece. Preliminary photocatalysis disinfection experiments were carried out on this matrix to explore optimum process parameters, including the optimal pre-treatment process of LD, TiO_2 concentration, and retention time. In addition, we explored PNFR, where nanofiltration and photocatalysis act simultaneously and in a synergetic way, to disinfect LD. This work sets the basis for the efficient operation and engineering application of a technology collaboration with photocatalysis as the final step for LD sanitation and reusable water recovery.

2. Materials and Methods

2.1. Liquid digestate origin, photocatalyst and pure cultures

LD was collected from various biogas plants, mostly sited in northern Greece, using various types of feedstocks during the last three years. The majority of these plants used cow manure as their main feedstock comprising 70-80% of the whole. The photocatalyst used was P25 TiO_2 (Degussa-Hüls AG, Frankfurt, Germany). Pathogens were added to the form of acclimatised pure cultures from certified reference materials (Sigma-Aldrich, Burlington, MA, USA) that were rehydrated in Maximum Recovery Diluent (Oxoid, Wesel, Germany), incubated overnight at 37 °C to reach maximum density and acclimatized another 24 to 48 hours at 37 °C in the LD material in use.

2.2. Determination of physical and chemical parameters

The quantification of physicochemical parameters involved several analytical methods and instruments. Total solids (TS), total suspended solids (TSS), and total dissolved solids (TDS) were determined by subjecting the samples to drying at 103 ± 2 °C and 180 ± 2 °C respectively, employing APHA method 2540 – B [54]. Volatile solids (VS), which

 doi:10.20944/preprints202305.2203.v1

represent the portion of suspended or dissolved solids lost from a sample upon ignition at a specified temperature for a specified duration, were determined following method APHA 2540-E [54]. Chemical Oxygen Demand (COD) refers to the amount of oxygen required for the chemical oxidation of organic constituents by a specific oxidant (dichromate ion, $Cr_2O_7^{2-}$) under controlled conditions and is expressed as oxygen equivalence. Analysis of COD was conducted using a commercial spectrometer, HACH DR 3900 (HACH, Loveland, CO, USA), as described [55]. pH values were measured electrometrically using a Jenway 3520 instrument (Cole-Parmer Ltd., Vernon Hills, IL, USA) equipped with a universal pH measuring electrode (924 001) and a temperature measuring electrode (027 500), following the APHA 4500-H+ method [56]. Turbidity was analyzed using a UV–vis spectrophotometer, specifically the COD3 Plus Colorimeter (LaMotte, Chestertown, MD, USA), according to APHA method 2540-E [54]. Total phosphorus (TP) was determined using the Molybdovanadate method and Hach reagents, employing the HACH DR3900 spectrophotometer. Nitrite-nitrogen (N-NO2) concentration was determined spectrophotometrically at 543 nm using a JASCO V-630 Spectrophotometer (JASCO, Inc, Tokyo, Japan). Nitrate-nitrogen (N-NO3) concentration was determined based on the APHA 4500-NO3- Ultraviolet Spectrophotometric Screening Method, with measurements taken at 220 nm using a JASCO V-630 Spectrophotometer [57]. Ammonium-nitrogen (N-NH4) concentration was determined photometrically at 420 nm using a JASCO V-630 Spectrophotometer. For the determination of heavy metals, an Agilent 7850 ICP-MS equipped with SPS 4 autosampler, sample introduction ISIS 3 system and Mass Hunter 5.1 software (Agilent Technologies, Santa Clara, CA, USA) for data acquisition and processing, was employed, following the procedures outlined in ISO 17,294 Part I & II and APHA 3125 [58-60]. Finally, the K, Ca, Mg, and Fe, were analyzed by flame photometry using an AA-7000 atomic absorption spectrophotometer (Shimadzu, Kyoto, Japan).

2.3. Microbiological analyses of indicator pathogens

Each sample (25g) was homogenized in sterile Buffered Peptone Water (BIOKAR Diagnostics, Allonne, France) using a Stomacher BagMixer 400 P (INTERSCIENCE, Saint-Nom-la-Bretèche, France). Serial dilutions were prepared and inoculated in triplicate on Tryptic Soy Agar (TSA, BIOKAR Diagnostics, Allonne, France) to enumerate mesophilic counts after incubation at 37 °C for 24 h. The enumeration of *Enterococcus faecalis* is based on a combination of ISO 7899-2:2000-Detection and Enumeration of *Enterococci* in water and CEN-TR 16193:2013-Detection and quantification of *Escherichia coli* in sewage sludge, treated biowaste and soil. The initial dilution was prepared by weighing 10g (wet weight) and adding an appropriate amount of peptone saline solution (BIOKAR Diagnostics, Allonne, France) so that the final volume was 100g. The material was then mixed in the homogenizer (Stomacher BagMixer 400 P, INTERSCIENCE, Saint-Nom-la-Bretèche, France) for 90 seconds. The material was aliquoted into containers and centrifuged (1600 rpm, 3 min, 10±1 °C). The supernatant (1mL) was aseptically vacuum filtered through a 0.45µm Whatman membrane (Whatman, Maidstone, UK) and the membrane was placed in a Slanetz and Bartley (SB, BIOKAR Diagnostics, Allonne, France) plate. The plates were incubated inverted at 36 ± 2 °C for 44 ± 4 hours. Decimal dilutions of the samples were filtered accordingly. After incubation if typical colonies (brown – red color) had developed, the membrane was transferred to Bile aesculin azide agar medium (BIOKAR Diagnostics, Allonne, France), which had been preheated to 44 ± 0.5 °C, as a confirmatory step. Black color development on Bile aesculin azide agar after 2 hours at 44 ± 0.5 °C indicates E. faecalis colony. Method efficiency (precision and trueness) testing was performed by measurements on laboratory inoculated suspension material containing the certified reference material *Enterococcus faecalis* WDCM 00,009 Vitroids (Sigma-Aldrich, Burlington, MA, USA). Samples were enumerated for *Escherichia coli* bacterial colonies (test portion=1 ml) by method ISO 16193: 2013-E. coli in Sludge (cultivation in Membrane Lactose Glucoronide Agar, MLGA, medium) and method ISO 9308-1:2014-E. coli in liquids waste

 doi:10.20944/preprints202305.2203.v1

(cultivation in Coliforms Chromogenic Agar, CCA, medium). For the detection of the *Salmonella* spp., the ISO 6579-1:2017 method was used (test portion=25 ml, Pre-enrichment with Buffered Peptone Water, BPW, and culture in Xylose Lysine Deoxycholate agar, XLD, nutrient selective medium). Colonies with typical *Salmonella* morphology were confirmed with real-time PCR after DNA extraction from the suspected colonies (StarPrep One kit, Salmonella Detection Lyokit, Biotecon Diagnostics, Potstdam, Germany). For the detection of *Listeria monocytogenes*, the ISO 11290-1:2017 standard was used (test portion= 25g sample, pre-enrichment in Fraser Broth Half concentration at 30 °C for 24 h, second enrichment in Fraser Base Broth (Oxoid, Wesel, Germany) at 30 °C for 24 h, and inoculation on Listeria Palcam Agar Base and ALOA Agar (Oxoid, Wesel, Germany). Colonies with typical *Listeria* morphology were confirmed as *L. monocytogenes* by real-time PCR after DNA extraction from the suspected colonies (StarPrep Two kit, L. monocytogenes Detection Lyokit, Biotecon Diagnostics, Potstdam, Germany). The results of *Salmonella* spp. and *L. monocytogenes* contamination were expressed as the presence/absence of pathogens. The enumeration of *Clostridium perfringens* performed according to ISO 7937:2004 on Tryptose Sulphite Cycloserine Agar (TSC, BIOKAR Diagnostics, Allonne, France) after anaerobic incubation at 42 °C for 24 h. Three to five suspected colonies (Gram-negative, catalase-negative) were confirmed with a reverse CAMP test. Briefly, cultures were inoculated at right angles within 1 to 2 mm of a β-haemolytic group B *Streptococcus* streak on Sheep Blood Agar plates (Biolife, Milan, Italy). After anaerobic incubation (37 °C for 18–24 h), a positive reverse CAMP test showed a "bow-tie" or "reverse arrow" pattern of hemolysis at the junction of the two cultures. Porcine Parvovirus testing was performed by virus DNA extraction with QIAamp DNA Mini kit (QIAGEN, Hilde, Germany) and quantification with the ViroReal Kit Porcine Parvovirus (Ingenetix, Wien, Austria), according to the manufacturers' instructions.

2.4. Pre-treatment of LD

LD was cooling centrifuged (4 °C) for 20 minutes at 3900g with Eppendorf 5810R (Eppendorf, Hamburg, Germany). Flocculants $FeCl_2$ (Ferrosol 90) or $FeCl_3$ (Ferrisol 100) or $FeClSO_4$ (Ferrisol 123) were added into the centrifuged samples at dosages of 3.5 g/L. The mixed samples were placed on a magnetic stirrer (HJ-6A, Jintan Kexi Instrument Co., Ltd, China) and stirred at a speed of 500 r/min for 3 min, then stirred at a speed of 60 r/min for 20 min. After standing for 2 h, vacuum filtration from glass fiber filters were made using the grades GF-3 and GF-5 (CHMLAB Group, Barcelona, Spain).

2.5. Photocatalysis experiments

Lab scale experiments were conducted as described elsewhere [61] with minor modifications. Briefly, as shown in Figure 1A, a 1L jacketed 5340-18 beaker (Ace Glass, Inc., Vineland, NJ, USA) with internal diameter 91 mm, and internal height 175 mm, was filled with 500mL material and was placed on the magnetic stirrer. A radiation source (OSRAM DULUX BLUE UVA 78 COLOR, 9W) was immerged using a quartz tube (35mm diameter) in the middle of the beaker (approximately 22mm from the bottom). A polypropylene cap was specially designed to hold the quartz tube in place. The cooling circulating pump was connected to the double-layer beaker to maintain a constant temperature at 25±1 °C. The device was then placed in a dark box.

Preprints (www.preprints.org) | NOT PEER-REVIEWED | Posted: 31 May 2023 doi:10.20944/preprints202305.2203.v1

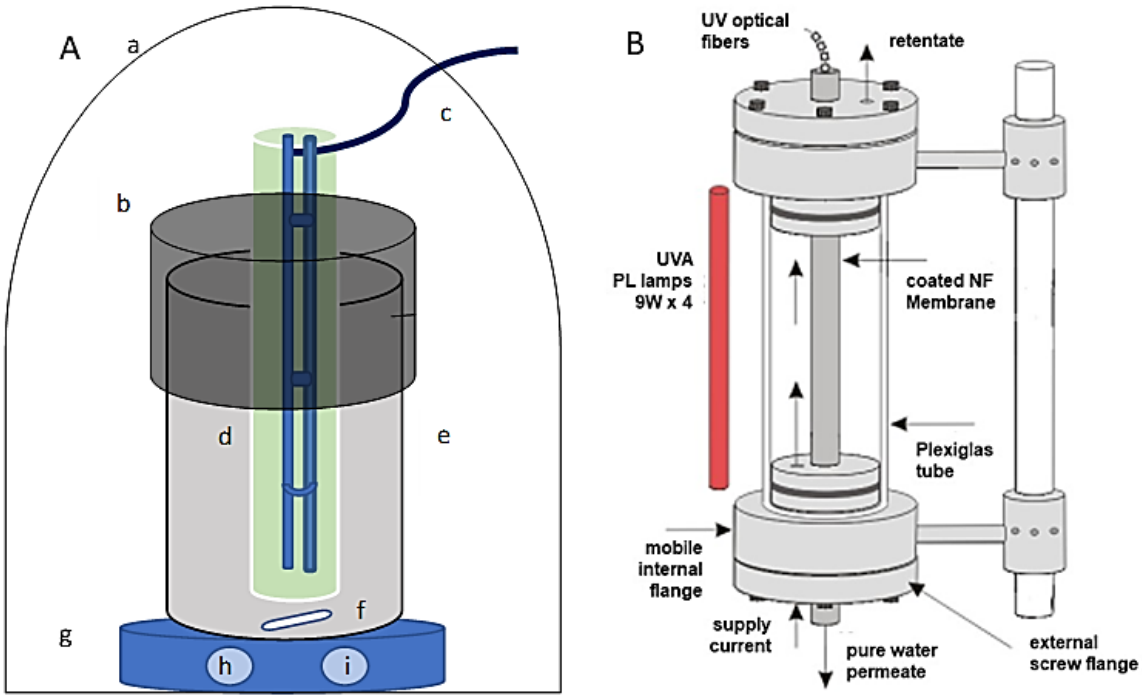

Figure 1. A, Graphical representation of the experimental photocatalysis setup (a) blackout cloth (b) black plastic cap on which the quartz tube stands (c) lamp, OSRAM DULUX BLUE UVA 78 COLOR, 9W (d) quartz tube (e) 1L jacketed beaker (f) stirring magnet (g) magnetic stirrer with temperature stabilizer (h) stirring intensity adjustment (i) temperature adjustment. B, Photocatalytic nanofiltration reactor arrangement.

The lab scale PNFR used in this study described in detail previously [62, 63]. This reactor consisted of one coated monolith and was equipped with appropriate flow and pressure control and illumination systems (Figure 1B). The transformation of the membrane monolith to photocatalytic membrane monolith was achieved by employing a simple and scalable wash-coating technique, which was based on a previously described method, adapted to our needs, and optimized via slight modifications [64]. In brief, 30 mmol of titanium (IV) isopropoxide (TTIP) were slowly added to 0.4 L of double-distilled water, at 40 °C. Then, concentrated HNO_3 (15mmol) was added dropwise under vigorous stirring at 80 °C, in order to catalyze the TTIP hydrolysis and obtain a transparent TiO_2 colloidal solution after 16 h. Hence, the overall reaction, including the hydrolysis and condensations steps of the titanium precursor (TTIP) for TiO_2 production, is summarized by the following equation:

$$Ti(OCH(CH_3)_2)_4 \rightarrow TiO_2 + 4CH_3CH_2CH_2OH \quad (1)$$

Once the sol was cooled down to room temperature, the commercial titania photocatalyst Evonik P25 Aeroxide (20g) was gradually added, and the resulting suspension was stirred overnight until homogenization. Finally, the membranes' modification was performed via the monolith immersion into the photocatalyst's slurry for 10 min and a subsequent annealing step at 150 °C overnight, employing custom-made lab furnaces.

3. Results and Discussion

 doi:10.20944/preprints202305.2203.v1

3.1. Characterization of LD

Table 1 presents the main LD characteristics obtained after AD of various feedstocks. The table shows that the main WD parameters can vary greatly, depending on both the type of substrate used in anaerobic fermentation and the AD process conditions. Especially, these variations are related to the input materials, which are usually classified as agri-food and livestock waste. In addition, the origin and the season of the input material could be important because, for example, the aerial deposition of heavy metals is usually higher in urban environments than in rural regions, while the deposition of heavy metals tends to peak in winter [49].

Table 1. Main LD characteristics obtained after AD of different feedstocks.

Parameter	Unit	Min-max values	Average	Standard Deviation
EC	mS/m	318-1880	650	626
pH	-	7.9-8.6	8.2	0.2
TS	%	1.32-5.83	3.22	1.6
VS	%	0.65-5.72	1.9	1.6
COD	mg/L	21333-42615	33800	809
TN	%	0.2-0.44	0.33	0.08
TP	%	0.01-0.14	0.04	0.05
N-NO3	%	0.002-0.01	0.006	0.003
N-NH4	%	0.13-0.36	0.22	0.06
Ca	%	0.014-0.14	0.044	0.05
K	%	0.12-0.35	0.24	0.08
Mg	%	0.007-5.1	0.04	1.9
Fe	%	0.004-0.022	0.008	0.007
Mn	%	0.00014-0.002	0.0006	0.0007
Na	%	0.07-0.16	0.09	0.03
Cl	%	0.14-1.19	0.35	0.39
Cd	mg/kg TS	<0.3-0.4	0.34	0.05
Cr	mg/kg TS	<8.3-14.6	7.5	3.8
Pb	mg/kg TS	<1-2.6	<1	-
Zn	mg/kg TS	209-1220	504	374
As	mg/kg TS	<3-15.15	<3	-
Cu	mg/kg TS	59-449	197	135
Hg	mg/kg TS	-	<0,02	-
Ni	mg/kg TS	11-30.3	17.1	7.1
E. coli	cfu/g	<10-13,000	-	-
E. faecalis	cfu/g	<10-250,000	-	-

3.2. Configuration of Photocatalytic Disinfection

After confirming the effectiveness of the photocatalytic arrangements with inoculated water samples (data not shown), we proceeded with various experiments to find out the working concentration of TiO_2 and the best pre-treatment approach. Untreated LD was disinfected after 70 hours of photocatalysis whereas 1:10 diluted WD was managed to be disinfected after approximately 30 hours (data not shown). None of the above results seems to be industrially applicable. The long disinfection time is attributed to the nature of the material as the light could not be transmitted effectively. Further dilution, on the other hand, conflicts with the purpose of the technology, which is to retrieve clean water and enhance circular economy of the biogas operation. So, we engage technologies that

Preprints (www.preprints.org) | NOT PEER-REVIEWED | Posted: 31 May 2023 doi:10.20944/preprints202305.2203.v1

are industrially applicable trying to remove the excess of total solid content and make LD translucent. Table 2 summarizes the physicochemical properties of the LD after each stage of selected pre-treatment (A-C) and the treatments (Di-Diii).

Table 2. Physicochemical and biological characteristics of LD, untreated (A), after centrifugation of A (B), after flocculation and μfiltration of B (C), after nanofiltration alone of C (Di), after 5.5h photocatalysis with 0.7g/L of C (Dii), and after PNFR of C (Diii).

		A: Untreated		B: Centrifuged		C: μFiltration		Di: nFiltation		Dii: Photocatalysis		Diii: PNFR	
Parameter	**Unit**	**Average**	**SD**	**Average**	**SD**	**Average**	**SD**	**Average**	**SD**	**Average**	**SD**	**Average**	**SD**
pH	-	8.14	0.11	8.20	0.10	8.50	0.12	8.50	0.10	8.30	0.10	8.20	0.10
EC	*mS/m*	534	18	550	26	645	30	415	41	520	28	284	27
TS	*%*	3.94	0.21	1.91	0.01	0.36	0.00	0.17	0.00	0.20	0.00	0.11	0.00
N-NH4	*mgN/L*	2881	267	2151	250	<0.1	n.a.	<0.1	n.a.	<0.1	n.a.	<0.1	n.a.
N	*%*	0.42	0.02	0.30	0.00	0.08	0.00	0.02	0.00	0.02	0.00	0.02	0.00
Cl	*mg/L*	2941	310	3900	607	745	99	672	192	520	144	481	151
Salinity	*‰*	3.22	0.11	3.26	0.17	4.40	0.10	2.50	0.10	3.15	0.10	2.50	0.10
N-NO3	*mgN/L*	60.93	12.95	43.50	8.00	<0.01	n.a.	<0.01	n.a.	<0.01	n.a.	<0.01	n.a.
VS	*%*	2.43	0.16	0.92	0.03	0.10	n.a.	<0.1	n.a.	<0.1	n.a.	<0.1	n.a.
P	*g/kg*	0.61	0.00	0.11	0.00	<0.1	n.a.	<0.1	n.a.	<0.1	n.a.	<0.1	n.a.
COD	*mgO2/L*	33750	4431	14280	1966	1190	190	732	35	417	20	298	22
TSS	*mg/L*	28000	9528	1775	159	180	33	61	1.00	33	1.22	4	0.01
Turbitity	*NTU*	n.a.*	n.a.	8000	244	1687	321	1100	208	477	132	248	75
E. coli	*cfu/g*	3250	3718	743	405	<10	n.a.	<10	n.a.	<10	n.a.	<10	n.a.
E. faecalis	*cfu/g*	3173	3217	2390	2492	410	53	<10	n.a.	<10	n.a.	<10	n.a.
C. perfrigens	*cfu/g*	4440	3526	3270	2873	300	130	<10	n.a.	<10	n.a.	<10	n.a.

*n.a., not applicable.

Figure 2A illustrates the disinfection rates in the pre-treated LD (see Table 1: C) that was inoculated with pure, fully developed culture of *E. faecalis* previously acclimatized in the material, using different TiO_2 concentrations and different retention times under UVA illumination. A sample without photocatalyst added served as control. The indicator organism used for preliminary experiments was *E. faecalis* which was found to be a constant and persistent pathogen in digestate samples.

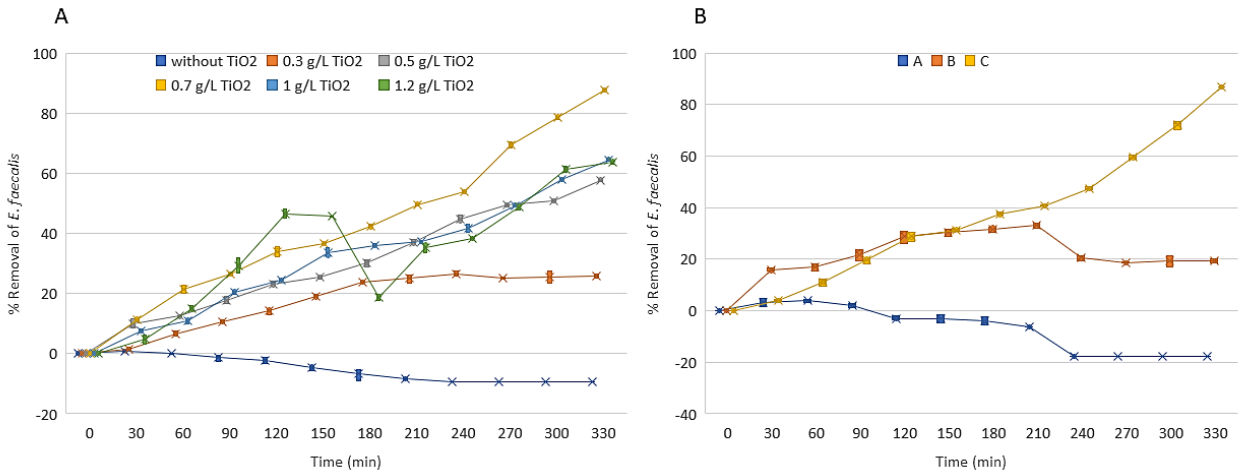

 doi:10.20944/preprints202305.2203.v1

Figure 2. (A) Disinfection rates under different concentrations of TiO2 under UVA illumination. (B) Pre-treatment dynamics on photocatalytic disinfection. A, untreated; B, centrifuged; C, flocculated and μFiltrated.

By increasing the dosage of TiO_2, more reactive species were produced, and pathogen removal was enhanced. However, high TiO_2 dosage can cause radiation scattering and the specific activity of TiO_2 is reduced. In addition, agglomeration of particles at high dosage interferes with the homogeneous structure of suspension and, as a result, the number of active sites on TiO_2 is decreased [65]. Based on these results, for all subsequent experiments, a TiO_2 concentration of 0.7 g/L was selected. This concentration succeeded sanitation to the maximum extent that can be measured by the selected method, which is 87.8% in 5.5h better than others implemented ($p<0,001$). It is worth noting that the removal of pathogens increased to 46.2% after 2h, when the TiO_2 concentration increased to 2.0 g/L but dropped to 18.8% at the third hour. This can be attributed to the increase of available adsorption of pathogens by TiO_2 [32]. The pre-treatment dynamics on photocatalytic disinfection using 0.7 g/L TiO_2 under UVA illumination is showed in Figure 2B. LD samples were used as indicated in Table 1 (A) untreated, (B) centrifuged, and (C) flocculated and μFiltrated. As expected, further pre-treatment enhances the disinfection effect.

There is significant debate regarding the specific processes or the combination of processes responsible for the death of microorganisms when they are exposed to photocatalytic action [66]. In general, the generated ROS, particularly hydroxyl radicals, exhibit strong oxidative power. They can attack the cellular components of pathogens, including lipids, proteins, and DNA. The ROS induce oxidative stress, leading to the destruction of the pathogens' cell membrane, inactivation of enzymes, and damage to genetic material. These processes disrupt the vital functions of the microorganisms and, ultimately, lead to their death or inability to replicate. The majority of literature agrees that inactivation starts and requires cell membrane degradation [67, 68]. However, injured bacteria may be temporarily inactivated. If bacteria are not completely harmed, they may enter a state where they are still viable but unable to grow in culture, and they can regain their ability to grow under more favourable conditions in the absence of light [69, 70]. To assess the impact of photocatalysis on common digestate pathogens, we conducted viability measurements of the pathogens after a two-hour period in darkness to ensure the absence of regrowth and to verify the efficacy of our system in achieving sanitized material (Figure 3).

 doi:10.20944/preprints202305.2203.v1

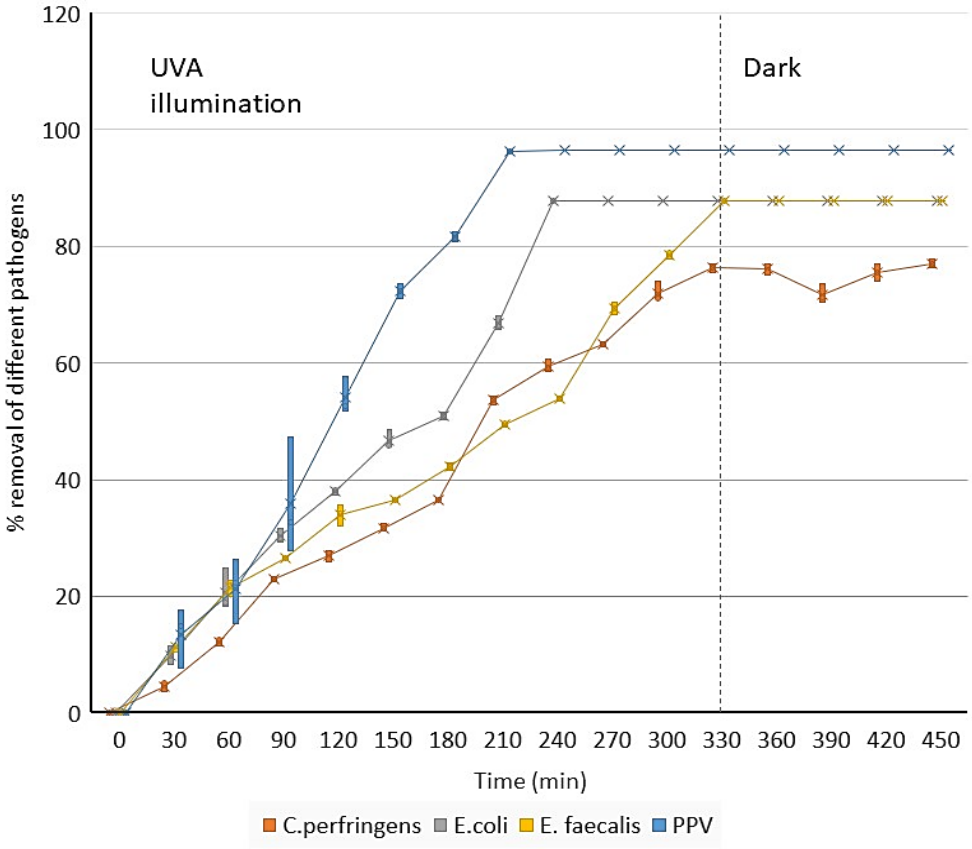

Figure 3. Photocatalytic disinfection of various pathogens using 0.7g/L TiO_2 under UVA illumination. The efficacy of the disinfection process was confirmed by maintaining the pathogen-free state for a duration of two hours in the absence of light.

Clostridium perfringens, a spore-forming bacterium, was found more resistant to photocatalysis compared to the others examined. Porcine parvovirus (PPV) was found more susceptible to the process compared to others, followed by *E. coli* and *E. faecalis.* Qualitative results of *Salmonella* spp. and *L. monocytogenes* showed absence of these pathogens after 5.5h (data not shown). *Listeria monocytogenes* is generally considered more resistant to photocatalysis compared to other bacteria, due to its ability to survive in harsh environmental conditions and its capacity to form biofilms [71]. All experiments operated under a stable temperature of 25±1°C using, as mentioned, a cooling system and temperature monitoring. Further evaluation of additional pathogens, such as *Clostridium botulinum*, *Clostridium tetani*, *Clostridioides difficile*, *Bacillus anthracis*, and *Bacillus cereus*, is needed. These microorganisms are frequently encountered in manure and are able to sporulate, exhibiting remarkable resilience, as they are resistant to a range of physical, chemical, and biological treatment methods [72].

3.3. PNFR implementation

Inoculated pre-treated LD with acclimatized full-grown cultures of pathogens passed through PNFR (Figure 4). In order to execute the experimental procedure, a continuous operation for a duration of 8 hours was necessitated. The laboratory reactor was subjected to an influx of 600 milliliters of feed over a time period of 40 minutes, followed by the generation of approximately 40 milliliters of filtrate within 30 minutes, while being exposed to pressure conditions of 8 bar. The time intervals labeled as t1-t3 correspond to

Preprints (www.preprints.org) | NOT PEER-REVIEWED | Posted: 31 May 2023 doi:10.20944/preprints202305.2203.v1

experimental conditions conducted in the absence of light, using the coated nanofiltration monolith. The observed reductions in microbial populations during these intervals can be attributed to the adsorption of microbes onto the membrane and nanofiltration mechanisms based on membrane porosity. The retentate line represents the concentrated fraction that did not pass through the membrane, while the permeate line represents the filtered fraction. On the other hand, intervals t4-t6 represent the results obtained when photocatalysis was employed, where the reactor operated under UV irradiation. It can be observed that, starting from interval t4, there was a decrease in microbial load, as well as in the concentrate fraction. This outcome verifies the effectiveness of the photocatalytic reactor as an environmentally friendly solution for waste treatment. Nevertheless, PNFR should be further optimized to treat LD, as we observed leakage phenomena attributed to chemical interactions with the membrane material. Mitigating or preventing membrane leakage is a significant concern in membrane-based technologies, and efforts are made to optimize membrane materials, design, and operating conditions to minimize or eliminate unintended substance transport across the membrane. No statistically significant changes were observed in the chemical parameters of the initial sample (feed), as indicated in Table 1 (Diii).

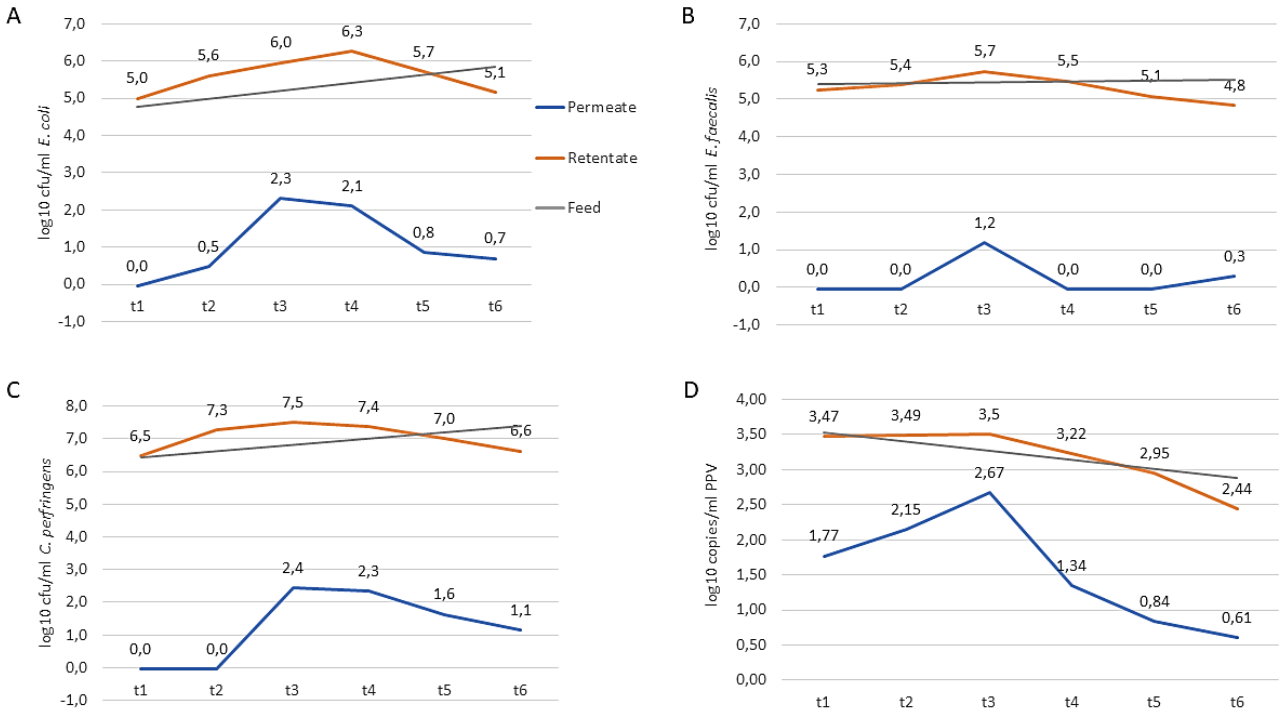

Figure 4. PNFR implementation for disinfection of pre-treated LD. (A) *E. coli*; (B) *E. faecalis*; (C) *C. perfringens*; (D) PPV.

4. Conclusions

The primary objectives of WD treatment encompass two key aspects: (i) the reduction of volume to enhance manageability and lower transportation costs, and (ii) the extraction of nutrients in a concentrated form. In general, WD treatment methods can be categorized into two distinct approaches: (a) Partial treatment, which focuses on reducing the volume or segregating it into solid and liquid components that are easier to handle or store. This

 doi:10.20944/preprints202305.2203.v1

step is typically undertaken as the initial phase of WD treatment, and it demands less energy and is comparatively more cost-effective than (b) complete purification. In the case of complete purification, valuable constituents are isolated and concentrated, while the remaining liquid fraction is purified to enable reuse in the AD process or direct discharge into a water body [73, 74]. In this research endeavor, our objective was to achieve the retention of pure water from liquid digestate, while simultaneously ensuring effective disinfection of the remaining material using photocatalysis. Though the utilization of suspensions exhibits efficacy at the laboratory scale, its industrial application is not feasible. Prior treatment of the material to eliminate solid content is essential, and a minimum duration of 5 hours is required for efficient disinfection. Furthermore, it is crucial to ascertain the optimal concentration to prevent any adverse impact on light transmission within the solution. The results obtained from the inactivation tests with TiO_2 suspensions conducted on pre-treated and inoculated liquid digestate demonstrated a significant five-log reduction in common pathogens within the initial 5-hour period, with no regrowth of pathogens observed.

To explore a possible industrial application for this purpose, additional experimentation was carried out using a patented photocatalytic nanofiltration reactor. The anticipated outcome was the reduction of the microbial load in the filtrate fraction of the photocatalytic reactor, as the modified nanofiltration monolith alone, without the application of photocatalysis, is theoretically adequate for pathogen removal. A noteworthy finding from experiments conducted in the photocatalytic reactor was the reduction of the microbial load in the concentrate fraction, an outcome not observed in the absence of photocatalysis. This particular innovation of the photocatalytic reactor allows for the extraction of two purified fractions instead of the conventional membrane waste treatment protocols that yield only a single purified fraction. Nevertheless, further research is needed for the optimization of the photocatalytic nanofiltration membranes for liquid digestate purification.

Author Contributions: Conceptualization, T.S., P.F., G.R., and A.G.C.; methodology, P.F., G.R., T.S. and A.G.C.; software, A.G.C..; validation, T.S., A.G.C.; formal analysis, A.G.C.; investigation, A.G.C., E.K, V.T.; resources, T.S.; data curation, A.G.C., T.S. and E.K.; writing—original draft preparation, A.G.C and G.S. ; writing—review and editing, A.G.C., T.S, G.R., V.T., E.K and P.F.; visualization, A.G.C.; supervision, T.S., G.R. and P.F..; project administration, T.S.; funding acquisition, T.S., All authors have read and agreed to the published version of the manuscript.

Funding: This research was co-funded by the European Regional Development Fund of the European Union and Greek national funds through the Operational Program Competitiveness, Entrepreneurship, and Innovation, under the call RESEARCH - CREATE – INNOVATE (project code: T2EDK-04043).

Institutional Review Board Statement: Not applicable.

Informed Consent Statement: Not applicable.

Data Availability Statement: The data presented in this study are available, upon request, from the corresponding author.

Acknowledgments: The authors wish to acknowledge Biogas Lagada S.A. and Bioenergy Nigrita S.A., that provided the liquid digestate to be used for experimentations. The authors also wish to acknowledge all staff members of Qlab P.C. for their individual roles that contributed to the implementation of this study, thank you Eleni Anna Economou, Ioanna Dalla, Nikoleta Prokopidou, Anastasia Manavi, Georgia Dimitropoulou, Ifigeneia Grigoriadou, Ioanna Christoforidou and Panagiotis Pantazis.

Conflicts of Interest: The authors declare that they have no known competing financial interests or personal relationships that could have appeared to influence the work reported in this paper.

References

1. Saravanan, A.; Kumar, P.S.; Nhung, T.C.; Ramesh, B.; Srinivasan, S.; Rangasamy, G. A review on biological methodologies in municipal solid waste management and landfilling: Resource and energy recovery. *Chemosphere* **2022**, *309*, doi:10.1016/j.chemosphere.2022.136630.
1. Pasalari, H.; Gholami, M.; Rezaee, A.; Esrafili, A.; Farzadkia, M. Perspectives on microbial community in anaerobic digestion with emphasis on environmental parameters: A systematic review. *Chemosphere* **2021**, *270*, doi:10.1016/j.chemosphere.2020.128618.
2. Uzinger, N.; Szecsy, O.; Szucs-Vasarhelyi, N.; Padra, I.; Sandor, D.B.; Loncaric, Z.; Draskovits, E.; Rekasi, M. Short-Term Decomposition and Nutrient-Supplying Ability of Sewage Sludge Digestate, Digestate Compost, and Vermicompost on Acidic Sandy and Calcareous Loamy Soils. *Agronomy-Basel* **2021**, *11*, doi:10.3390/agronomy11112249.
3. Kovacic, D.; Loncaric, Z.; Jovic, J.; Samac, D.; Popovic, B.; Tisma, M. Digestate Management and Processing Practices: A Review. *Applied Sciences-Basel* **2022**, *12*, doi:10.3390/app12189216.
4. Tambone, F.; Scaglia, B.; D'Imporzano, G.; Schievano, A.; Orzi, V.; Salati, S.; Adani, F. Assessing amendment and fertilizing properties of digestates from anaerobic digestion through a comparative study with digested sludge and compost. *Chemosphere* **2010**, *81*, 577-583, doi:10.1016/j.chemosphere.2010.08.034.
5. Peng, W.; Lu, F.; Hao, L.P.; Zhang, H.; Shao, L.M.; He, P.J. Digestate management for high-solid anaerobic digestion of organic wastes: A review. *Bioresource Technology* **2020**, *297*, doi:10.1016/j.biortech.2019.122485.
6. Hutchison, M.L.; Walters, L.D.; Avery, S.M.; Synge, B.A.; Moore, A. Levels of zoonotic agents in British livestock manures. *Letters in Applied Microbiology* **2004**, *39*, 207-214, doi:10.1111/j.1472-765X.2004.01564.x.
7. Johansson, M.; Emmoth, E.; Salomonsson, A.C.; Albihn, A. Potential risks when spreading anaerobic digestion residues on grass silage crops - survival of bacteria, moulds and viruses. *Grass and Forage Science* **2005**, *60*, 175-185, doi:10.1111/j.1365-2494.2005.00466.x.
8. Goberna, M.; Podmirseg, S.M.; Waldhuber, S.; Knapp, B.A.; Garcia, C.; Insam, H. Pathogenic bacteria and mineral N in soils following the land spreading of biogas digestates and fresh manure. *Applied Soil Ecology* **2011**, *49*, 18-25, doi:10.1016/j.apsoil.2011.07.007.
9. Smith, S.R.; Lang, N.L.; Cheung, K.H.M.; Spanoudaki, K. Factors controlling pathogen destruction during anaerobic digestion of biowastes. *Waste Management* **2005**, *25*, 417-425, doi:10.1016/j.wasman.2005.02.010.
10. Sfetsas, T.; Patsatzis, S.; Chioti, A.; Kopteropoulos, A.; Dimitropoulou, G.; Tsioni, V.; Kotsopoulos, T. A review of advances in valorization and post-treatment of anaerobic digestion liquid fraction effluent. *Waste Management & Research* **2022**, *40*, 1093-1109, doi:10.1177/0734242 × 211073000.
11. Erickson, M.C.; Ortega, Y.R. Inactivation of protozoan parasites in food, water, and environmental systems. *Journal of Food Protection* **2006**, *69*, 2786-2808, doi:10.4315/0362-028x-69.11.2786.
12. Liu, X.J.; Lendormi, T.; Lanoiselle, J.L. Conventional and Innovative Hygienization of Feedstock for Biogas Production: Resistance of Indicator Bacteria to Thermal Pasteurization, Pulsed Electric Field Treatment, and Anaerobic Digestion. *Energies* **2021**, *14*, doi:10.3390/en14071938.
13. Seruga, P.; Krzywonos, M.; Paluszak, Z.; Urbanowska, A.; Pawlak-Kruczek, H.; Niedzwiecki, L.; Pinkowska, H. Pathogen Reduction Potential in Anaerobic Digestion of Organic Fraction of Municipal Solid Waste and Food Waste. *Molecules* **2020**, *25*, doi:10.3390/molecules25020275.
14. Liu, X.J.; Lendormi, T.; Lanoiselle, J.L. Overview of hygienization pretreatment for pasteurization and methane potential enhancement of biowaste: Challenges, state of the art and alternative technologies. *Journal of Cleaner Production* **2019**, *236*, doi:10.1016/j.jclepro.2019.06.356.
15. Froschle, B.; Heiermann, M.; Lebuhn, M.; Messelhausser, U.; Plochl, M. Hygiene and Sanitation in Biogas Plants. In *Biogas Science and Technology*, Guebitz, G.M., Bauer, A., Bochmann, G., Gronauer, A., Weiss, S., Eds.; Advances in Biochemical Engineering-Biotechnology; 2015; Volume 151, pp. 63-99.
16. Golovko, O.; Ahrens, L.; Schelin, J.; Sorengard, M.; Bergstrand, K.J.; Asp, H.; Hultberg, M.; Wiberg, K. Organic micropollutants, heavy metals and pathogens in anaerobic digestate based on food waste. *Journal of Environmental Management* **2022**, *313*, doi:10.1016/j.jenvman.2022.114997.
17. Lin, M.; Wang, A.J.; Ren, L.J.; Qiao, W.; Wandera, S.M.; Dong, R.J. Challenges of pathogen inactivation in animal manure through anaerobic digestion: a short review. *Bioengineered* **2022**, *13*, 1149-1161, doi:10.1080/21655979.2021.2017717.
18. Bagge, E.; Persson, M.; Johansson, K.E. Diversity of spore-forming bacteria in cattle manure, slaughterhouse waste and samples from biogas plants. *Journal of Applied Microbiology* **2010**, *109*, 1549-1565, doi:10.1111/j.1365-2672.2010.04790.x.
19. Le Marechal, C.; Druilhe, C.; Reperant, E.; Boscher, E.; Rouxel, S.; Le Roux, S.; Poezevara, T.; Ziebal, C.; Houdayer, C.; Nagard, B.; et al. Evaluation of the occurrence of sporulating and nonsporulating pathogenic bacteria in manure and in digestate of five agricultural biogas plants. *Microbiologyopen* **2019**, *8*, doi:10.1002/mbo3.872.
20. Pulvirenti, A.; Ronga, D.; Zaghi, M.; Tomasselli, A.R.; Mannella, L.; Pecchioni, N. Pelleting is a successful method to eliminate the presence of Clostridium spp. from the digestate of biogas plants. *Biomass & Bioenergy* **2015**, *81*, 479-482, doi:10.1016/j.biombioe.2015.08.008.
21. Galedari, M.; Ghazi, M.M.; Mirmasoomi, S.R. Photocatalytic process for the tetracycline removal under visible light: Presenting a degradation model and optimization using response surface methodology (RSM). *Chemical Engineering Research & Design* **2019**, *145*, 323-333, doi:10.1016/j.cherd.2019.03.031.

22. Al-Hamdi, A.M.; Rinner, U.; Sillanpaa, M. Tin dioxide as a photocatalyst for water treatment: A review. *Process Safety and Environmental Protection* **2017**, *107*, 190-205, doi:10.1016/j.psep.2017.01.022.
23. Rivera-Utrilla, J.; Sanchez-Polo, M.; Ferro-Garcia, M.A.; Prados-Joya, G.; Ocampo-Perez, R. Pharmaceuticals as emerging contaminants and their removal from water. A review. *Chemosphere* **2013**, *93*, 1268-1287, doi:10.1016/j.chemosphere.2013.07.059.
24. Rimoldi, L.; Meroni, D.; Cappelletti, G.; Ardizzone, S. Green and low cost tetracycline degradation processes by nanometric and immobilized TiO2 systems. *Catalysis Today* **2017**, *281*, 38-44, doi:10.1016/j.cattod.2016.08.015.
25. Liu, Y.Q.; He, X.X.; Duan, X.D.; Fu, Y.S.; Fatta-Kassinos, D.; Dionysiou, D.D. Significant role of UV and carbonate radical on the degradation of oxytetracycline in UV-AOPs: Kinetics and mechanism. *Water Research* **2016**, *95*, 195-204, doi:10.1016/j.watres.2016.03.011.
26. M'Arimi, M.M.; Mecha, C.A.; Kiprop, A.K.; Ramkat, R. Recent trends in applications of advanced oxidation processes (AOPs) in bioenergy production: Review. *Renewable & Sustainable Energy Reviews* **2020**, *121*, doi:10.1016/j.rser.2019.109669.
27. Wu, S.Q.; Hu, H.Y.; Lin, Y.; Zhang, J.L.; Hu, Y.H. Visible light photocatalytic degradation of tetracycline over TiO2. *Chemical Engineering Journal* **2020**, *382*, doi:10.1016/j.cej.2019.122842.
28. Wang, H.; Wang, H.L.; Jiang, W.F. Solar photocatalytic degradation of 2,6-dinitro-p-cresol (DNPC) using multi-walled carbon nanotubes (MWCNTs)-TiO2 composite photocatalysts. *Chemosphere* **2009**, *75*, 1105-1111, doi:10.1016/j.chemosphere.2009.01.014.
29. Wang, P.P.; Yuan, Q.X. Photocatalytic degradation of tetracyclines in liquid digestate: Optimization, kinetics and correlation studies. *Chemical Engineering Journal* **2021**, *410*, doi:10.1016/j.cej.2020.128327.
30. Wang, P.P.; Xu, C.; Zhang, X.; Yuan, Q.X.; Shan, S.D. Effect of photocatalysis on the physicochemical properties of liquid digestate. *Environmental Research* **2023**, *223*, doi:10.1016/j.envres.2023.115467.
31. Yin, F.B.; Lin, S.Y.; Zhou, X.Q.; Dong, H.M.; Zhan, Y.H. Fate of antibiotics during membrane separation followed by physical-chemical treatment processes. *Science of the Total Environment* **2021**, *759*, doi:10.1016/j.scitotenv.2020.143520.
32. Jin, X.D.; Zhou, X.Q.; Sun, P.; Lin, S.Y.; Cao, W.B.; Li, Z.F.; Liu, W.X. Photocatalytic degradation of norfloxacin using N-doped TiO2: Optimization, mechanism, identification of intermediates and toxicity evaluation. *Chemosphere* **2019**, *237*, doi:10.1016/j.chemosphere.2019.124433.
33. Hu, X.; Hu, X.J.; Peng, Q.Q.; Zhou, L.; Tan, X.F.; Jiang, L.H.; Tang, C.F.; Wang, H.; Liu, S.H.; Wang, Y.Q.; et al. Mechanisms underlying the photocatalytic degradation pathway of ciprofloxacin with heterogeneous TiO2. *Chemical Engineering Journal* **2020**, *380*, doi:10.1016/j.cej.2019.122366.
34. Huang, J.X.; Li, D.G.; Li, R.B.; Chen, P.; Zhang, Q.X.; Liu, H.J.; Lv, W.Y.; Liu, G.G.; Feng, Y.P. One-step synthesis of phosphorus/oxygen co-doped g-C3N4/anatase TiO2 Z-scheme photocatalyst for significantly enhanced visible-light photocatalysis degradation of enrofloxacin. *Journal of Hazardous Materials* **2020**, *386*, doi:10.1016/j.jhazmat.2019.121634.
35. Espindola, J.C.; Cristovao, R.O.; Mendes, A.; Boaventura, R.A.R.; Vilar, V.J.P. Photocatalytic membrane reactor performance towards oxytetracycline removal from synthetic and real matrices: Suspended vs. immobilized TiO2-P25. *Chemical Engineering Journal* **2019**, *378*, doi:10.1016/j.cej.2019.122114.
36. Devi, M.; Praharaj, S.; Rout, D. 20 - Industrial problems and solution towards visible light photocatalysis. In *Nanostructured Materials for Visible Light Photocatalysis*, Nayak, A.K., Sahu, N.K., Eds.; Elsevier: 2022; pp. 535-567.
37. He, J.H.; Kumar, A.; Khan, M.; Lo, I.M.C. Critical review of photocatalytic disinfection of bacteria: from noble metals- and carbon nanomaterials-TiO2 composites to challenges of water characteristics and strategic solutions. *Science of the Total Environment* **2021**, *758*, doi:10.1016/j.scitotenv.2020.143953.
38. Lofrano, G.; Ubaldi, F.; Albarano, L.; Carotenuto, M.; Vaiano, V.; Valeriani, F.; Libralato, G.; Gianfranceschi, G.; Fratoddi, I.; Meric, S.; et al. Antimicrobial Effectiveness of Innovative Photocatalysts: A Review. *Nanomaterials* **2022**, *12*, doi:10.3390/nano12162831.
39. Alrousan, D.M.A.; Dunlop, P.S.M.; McMurray, T.A.; Byrne, J.A. Photocatalytic inactivation of E. coli in surface water using immobilised nanoparticle TiO2 films. *Water Research* **2009**, *43*, 47-54, doi:10.1016/j.watres.2008.10.015.
40. Fernandes, F.; Silkina, A.; Fuentes-Grunewald, C.; Wood, E.E.; Ndovela, V.L.S.; Oatley-Radcliffe, D.L.; Lovitt, R.W.; Llewellyn, C.A. Valorising nutrient-rich digestate: Dilution, settlement and membrane filtration processing for optimisation as a waste-based media for microalgal cultivation. *Waste Management* **2020**, *118*, 197-208, doi:10.1016/j.wasman.2020.08.037.
41. Camilleri-Rumbau, M.S.; Soler-Cabezas, J.L.; Christensen, K.V.; Norddahl, B.; Mendoza-Roca, J.A.; Vincent-Vela, M.C. Application of aquaporin-based forward osmosis membranes for processing of digestate liquid fractions. *Chemical Engineering Journal* **2019**, *371*, 583-592, doi:10.1016/j.cej.2019.02.029.
42. Camilleri-Rumbau, M.S.; Norddahl, B.; Wei, J.; Christensen, K.V.; Sotoft, L.F. Microfiltration and ultrafiltration as a post-treatment of biogas plant digestates for producing concentrated fertilizers. *Desalination and Water Treatment* **2015**, *55*, 1639-1653, doi:10.1080/19443994.2014.989638.
43. Swiatczak, P.; Cydzik-Kwiatkowska, A.; Zielinska, M. Treatment of Liquid Phase of Digestate from Agricultural Biogas Plant in a System with Aerobic Granules and Ultrafiltration. *Water* **2019**, *11*, doi:10.3390/w11010104.
44. Yue, C.D.; Dong, H.M.; Chen, Y.X.; Shang, B.; Wang, Y.; Wang, S.L.; Zhu, Z.P. Direct Purification of Digestate Using Ultrafiltration Membranes: Influence of Pore Size on Filtration Behavior and Fouling Characteristics. *Membranes* **2021**, *11*, doi:10.3390/membranes11030179.
45. Adam, G.; Mottet, A.; Lemaigre, S.; Tsachidou, B.; Trouve, E.; Delfosse, P. Fractionation of anaerobic digestates by dynamic nanofiltration and reverse osmosis: An industrial pilot case evaluation for nutrient recovery. *Journal of Environmental Chemical Engineering* **2018**, *6*, 6723-6732, doi:10.1016/j.jece.2018.10.033.

46. Zhan, Y.H.; Yin, F.B.; Yue, C.D.; Zhu, J.; Zhu, Z.P.; Zou, M.Y.; Dong, H.M. Effect of Pretreatment on Hydraulic Performance of the Integrated Membrane Process for Concentrating Nutrient in Biogas Digestate from Swine Manure. *Membranes* **2020**, *10*, doi:10.3390/membranes10100249.
47. Blandin, G.; Ferrari, F.; Lesage, G.; Le-Clech, P.; Heran, M.; Martinez-Llado, X. Forward Osmosis as Concentration Process: Review of Opportunities and Challenges. *Membranes* **2020**, *10*, doi:10.3390/membranes10100284.
48. Oller, I.; Malato, S.; Sanchez-Perez, J.A. Combination of Advanced Oxidation Processes and biological treatments for wastewater decontamination-A review. *Science of the Total Environment* **2011**, *409*, 4141-4166, doi:10.1016/j.scitotenv.2010.08.061.
49. Falaras, P.; Romanos, G.; Aloupogiannis, P. Photocatalytic purification device. *Application number EP10275076* **2012**, *7*.
50. Pelaez, M.; Nolan, N.T.; Pillai, S.C.; Seery, M.K.; Falaras, P.; Kontos, A.G.; Dunlop, P.S.M.; Hamilton, J.W.J.; Byrne, J.A.; O'Shea, K.; et al. A review on the visible light active titanium dioxide photocatalysts for environmental applications. *Applied Catalysis B-Environmental* **2012**, *125*, 331-349, doi:10.1016/j.apcatb.2012.05.036.
51. Athanasekou, C.P.; Romanos, G.E.; Katsaros, F.K.; Kordatos, K.; Likodimos, V.; Falaras, P. Very efficient composite titania membranes in hybrid ultrafiltration/photocatalysis water treatment processes. *Journal of Membrane Science* **2012**, *392*, 192-203, doi:10.1016/j.memsci.2011.12.028.
52. Theodorakopoulos, G.V.; Arfanis, M.K.; Perez, J.A.S.; Aguera, A.; Aponte, F.X.C.; Markellou, E.; Romanos, G.E.; Falaras, P. Novel Pilot-Scale Photocatalytic Nanofiltration Reactor for Agricultural Wastewater Treatment. *Membranes* **2023**, *13*, doi:10.3390/membranes13020202.
53. 2540 SOLIDS. In *Standard Methods For the Examination of Water and Wastewater*.
54. 5220 CHEMICAL OXYGEN DEMAND (COD). In *Standard Methods For the Examination of Water and Wastewater*.
55. 4500-H⁺ pH. In *Standard Methods For the Examination of Water and Wastewater*.
56. 4500-NO₃[−] NITROGEN (NITRATE). In *Standard Methods For the Examination of Water and Wastewater*.
57. British Standards, I. *BS ISO 17294-1. Water quality. Application of inductively coupled plasma mass spectrometry (ICP-MS)*; British Standards Institution: London, 2022.
58. British Standards, I. *BS EN ISO 17294-2. Water quality. Application of inductively coupled plasma mass spectrometry (ICP-MS)*; British Standards Institution: London, 2022.
59. 3125 METALS BY INDUCTIVELY COUPLED PLASMA-MASS SPECTROMETRY. In *Standard Methods For the Examination of Water and Wastewater*.
60. Bojinova, A.; Kralchevska, R.; Poulios, I.; Dushkin, C. Anatase/rutile TiO2 composites: Influence of the mixing ratio on the photocatalytic degradation of Malachite Green and Orange II in slurry. *Materials Chemistry and Physics* **2007**, *106*, 187-192, doi:10.1016/j.matchemphys.2007.05.035.
61. Moustakas, N.G.; Katsaros, F.K.; Kontos, A.G.; Romanos, G.E.; Dionysiou, D.D.; Falaras, P. Visible light active TiO2 photocatalytic filtration membranes with improved permeability and low energy consumption. *Catalysis Today* **2014**, *224*, 56-69, doi:10.1016/j.cattod.2013.10.063.
62. Papageorgiou, S.K.; Katsaros, F.K.; Favvas, E.P.; Romanos, G.E.; Athanasekou, C.P.; Beltsios, K.G.; Tzialla, O.I.; Falaras, P. Alginate fibers as photocatalyst immobilizing agents applied in hybrid photocatalytic/ultrafiltration water treatment processes. *Water Research* **2012**, *46*, 1858-1872, doi:10.1016/j.watres.2012.01.005.
63. Du, P.; Cameiro, J.T.; Moulijn, J.A.; Mul, G. A novel photocatalytic monolith reactor for multiphase heterogeneous photocatalysis. *Applied Catalysis a-General* **2008**, *334*, 119-128, doi:10.1016/j.apcata.2007.09.045.
64. Bagge, E.; Sahlstrom, L.; Albihn, A. The effect of hygienic treatment on the microbial flora of biowaste at biogas plants. *Water Research* **2005**, *39*, 4879-4886, doi:10.1016/j.watres.2005.03.016.
65. Mecha, A.C.; Onyango, M.S.; Ochieng, A.; Momba, M.N.B. UV and solar photocatalytic disinfection of municipal wastewater: inactivation, reactivation and regrowth of bacterial pathogens. *International Journal of Environmental Science and Technology* **2019**, *16*, 3687-3696, doi:10.1007/s13762-018-1950-1.
66. Wang, W.; Huang, G.; Yu, J.C.; Wong, P.K. Advances in photocatalytic disinfection of bacteria: Development of photocatalysts and mechanisms. *Journal of Environmental Sciences* **2015**, *34*, 232-247, doi:10.1016/j.jes.2015.05.003.
67. Reddy, P.V.L.; Kavitha, B.; Reddy, P.A.K.; Kim, K.-H. TiO2-based photocatalytic disinfection of microbes in aqueous media: A review. *Environmental Research* **2017**, *154*, 296-303, doi:10.1016/j.envres.2017.01.018.
68. McCullagh, C.; Robertson, J.M.C.; Bahnemann, D.W.; Robertson, P.K.J. The application of TiO2 photocatalysis for disinfection of water contaminated with pathogenic micro-organisms: a review. *Research on Chemical Intermediates* **2007**, *33*, 359-375, doi:10.1163/156856707779238775.
69. Mecha, A.C.; Onyango, M.S.; Ochieng, A.; Momba, M.N.B. Evaluation of synergy and bacterial regrowth in photocatalytic ozonation disinfection of municipal wastewater. *Science of the Total Environment* **2017**, *601*, 626-635, doi:10.1016/j.scitotenv.2017.05.204.
70. Liu, N.; Ming, J.; Sharma, A.; Sun, X.; Kawazoe, N.; Chen, G.P.; Yang, Y.N. Sustainable photocatalytic disinfection of four representative pathogenic bacteria isolated from real water environment by immobilized TiO2-based composite and its mechanism. *Chemical Engineering Journal* **2021**, *426*, doi:10.1016/j.cej.2021.131217.
71. Subirats, J.; Sharpe, H.; Topp, E. Fate of Clostridia and other spore-forming Firmicute bacteria during feedstock anaerobic digestion and aerobic composting. *Journal of Environmental Management* **2022**, *309*, doi:10.1016/j.jenvman.2022.114643.
72. Plana, P.V.; Noche, B. A review of the current digestate distribution models: storage and transport. In Proceedings of the 8th International Conference on Waste Management and the Environment, Valencia, SPAIN, Jun 07-09, 2016; pp. 345-357.

 doi:10.20944/preprints202305.2203.v1

73. Fuchs, W.; Drosg, B. Assessment of the state of the art of technologies for the processing of digestate residue from anaerobic digesters. *Water Science and Technology* **2013**, *67*, 1984-1993, doi:10.2166/wst.2013.075.